

# Developmental Cell

## **Doublesex Regulates the Connectivity of a Neural Circuit Controlling *Drosophila* Male Courtship Song**

### Highlights

- *Doublesex*-expressing TN1 neurons are necessary and sufficient for the male sine song
- A subclass of TN1 neurons, TN1A, contributes to the sine song
- TN1A neurons are functionally coupled to a sine song motoneuron, *hg1*
- *Doublesex* regulates the connectivity between the TN1A and *hg1* neurons

### Authors

Troy R. Shirangi, Allan M. Wong,  
James W. Truman, David L. Stern

### Correspondence

shirangit@janelia.hhmi.org

### In Brief

It is unclear how developmental regulatory genes specify sex-specific behaviors. Shirangi et al. demonstrate that the *Drosophila* sexual differentiation gene *doublesex* encodes a sex-specific behavior—male song—by promoting the connectivity between the male-specific TN1A neurons and the sex-non-specific *hg1* neurons, which are required for production of the song.



# Doublesex Regulates the Connectivity of a Neural Circuit Controlling *Drosophila* Male Courtship Song

Troy R. Shirangi,<sup>1,\*</sup> Allan M. Wong,<sup>1</sup> James W. Truman,<sup>1</sup> and David L. Stern<sup>1</sup><sup>1</sup>Janelia Research Campus, Howard Hughes Medical Institute, 19700 Helix Drive, Ashburn, VA 20147, USA\*Correspondence: [shirangit@janelia.hhmi.org](mailto:shirangit@janelia.hhmi.org)<http://dx.doi.org/10.1016/j.devcel.2016.05.012>

## SUMMARY

It is unclear how regulatory genes establish neural circuits that compose sex-specific behaviors. The *Drosophila melanogaster* male courtship song provides a powerful model to study this problem. Courting males vibrate a wing to sing bouts of pulses and hums, called pulse and sine song, respectively. We report the discovery of male-specific thoracic interneurons—the TN1A neurons—that are required specifically for sine song. The TN1A neurons can drive the activity of a sex-non-specific wing motoneuron, *hg1*, which is also required for sine song. The male-specific connection between the TN1A neurons and the *hg1* motoneuron is regulated by the sexual differentiation gene *doublesex*. We find that *doublesex* is required in the TN1A neurons during development to increase the density of the TN1A arbors that interact with dendrites of the *hg1* motoneuron. Our findings demonstrate how a sexual differentiation gene can build a sex-specific circuit motif by modulating neuronal arborization.

## INTRODUCTION

Studies in mice, flies, and worms have shown that innate sexual differences in behavior are usually encoded during development by master regulatory genes that act as genetic switches between the male and the female state (Baker et al., 2001; Manoli et al., 2013, 2006; Portman, 2007). It is well established that these regulatory genes can mediate the dimorphic development of specific neurons or neural populations. However, how the activity of these genes influences the form and function of the neural circuits that compose sex-specific behaviors is poorly understood.

During courtship, a *Drosophila melanogaster* male will orient toward a female and vibrate a wing to produce a song consisting of trains of pulses called pulse song and bouts of continuous tone called sine song (Figure 1A). Two sex-specifically spliced transcription factors, *doublesex* (*dsx*) and *fruitless* (*fru*), are required to build the neural anatomy that enables male song (reviewed in Billeter et al., 2006). *dsx* and *fru* are expressed in about 1% and 2% of neurons, respectively, in the developing male nervous system (Lee et al., 2000, 2002; Manoli et al., 2005; Rideout et al., 2010; Robinett et al., 2010; Stockinger et al., 2005), and some of these neurons compose the circuitry required for song

(Rideout et al., 2007; von Philipsborn et al., 2011). Many of these neurons exhibit striking anatomical differences between the sexes (Cachero et al., 2010; Rideout et al., 2010; Robinett et al., 2010; Yu et al., 2010), but only recently have we begun to understand how these anatomical differences influence the structure and function of the circuits that generate courtship. For example, Kohl et al. (2013) demonstrated that *fru* acts to reposition dendritic arbors of third-order olfactory neurons in either male- or female-specific configurations, thereby routing sex-pheromone processing into either male- or female-specific courtship pathways, respectively.

Here, we describe the identification of a neural circuit element that generates sine song and show how *dsx* directs the physical and functional connectivity of this neural circuit. We identified a cluster of approximately 30 *dsx*-expressing interneurons, called TN1 (Lee et al., 2002), that are necessary for natural production of sine song and that, upon activation, can drive sine song. The TN1 neurons contribute to several aspects of courtship song, but at least one subtype of TN1 neurons, the TN1A neurons, mediate sine song specifically. The TN1A neurons are functionally coupled to a wing motoneuron, *hg1*, which we had previously reported is required for sine song (Shirangi et al., 2013). The functional connection between the TN1A neurons and the *hg1* motoneuron requires *dsx* expression in the TN1A cells. *dsx* acts in the TN1A neurons to increase the density of their arbors specifically where the dendrites of the *hg1* motoneuron reside. Our results illustrate that the sexual differentiation gene, *dsx*, facilitates the connectivity of a neural circuit motif by regulating neuronal arborization, thereby facilitating the production of a sex-limited motor behavior.

## RESULTS

### TN1 Neurons Are Necessary and Sufficient for the Singing of Sine Song

To identify neural circuit elements required for courtship song, we re-examined the observation by Vilella and Hall (1996) that courting males carrying mutations in the sexual differentiation transcription factor *doublesex* (*dsx*) could sing pulse song, but not sine song. We confirmed that *dsx* mutant males do not sing sine song (Figure 1B). *dsx* mutant males also sang less pulse song relative to heterozygote controls (Figure 1B), and displayed quantitative defects in the inter-pulse interval, the pulse carrier frequency, and the pulse amplitude (Figures 1C–1E).

Because the thoracic ventral nervous system drives rhythmic motor behaviors such as flying, walking, and singing, we hypothesized that these song defects resulted from loss of *dsx* activity

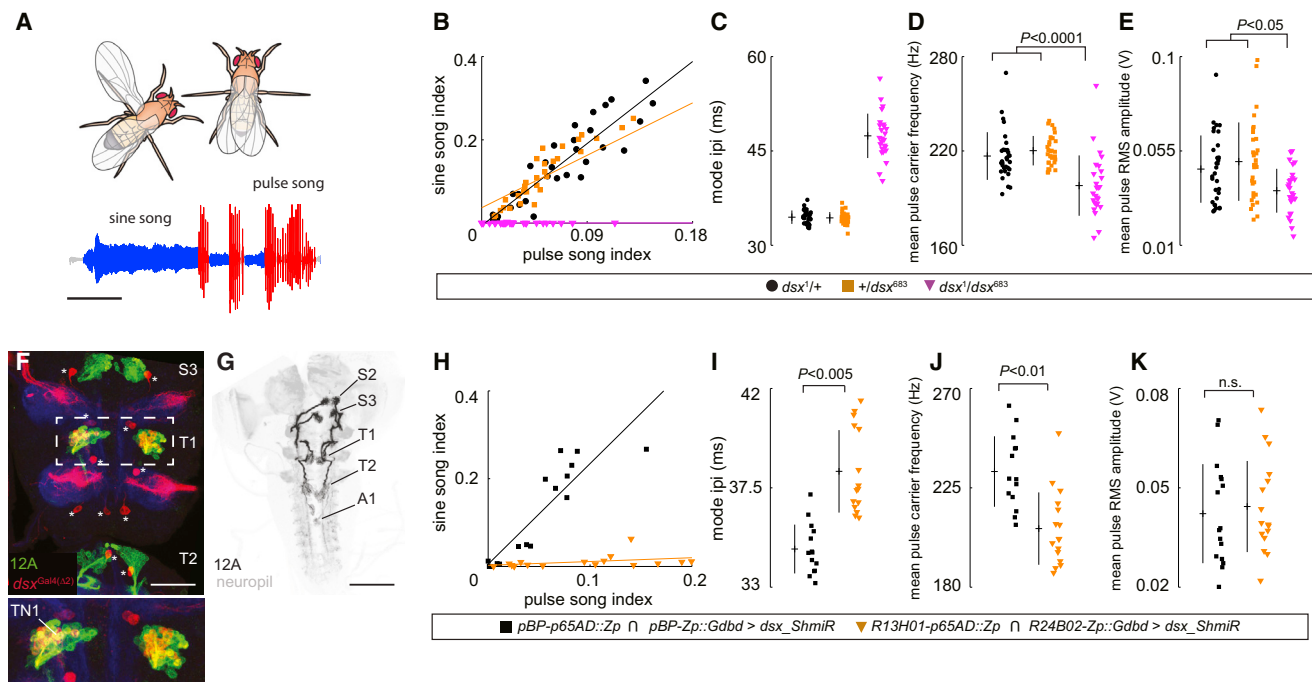


**Figure 1. *dsx* Influences *Drosophila* Male Courtship Song**

(A) *Drosophila melanogaster* male courtship song. Scale bar represents 1 s.

(B–E) Courting males with mutations in *dsx* (magenta) are unable to sing sine song, and sing pulse song with quantitative defects relative to heterozygote controls (orange and black). (B) The proportion of sine song amount relative to pulse song amount. To quantify the amount of pulse or sine song that a courting male sings, we measured the pulse and sine song index, which is the fraction of time the male spends singing pulse or sine song. (C) Mode inter-pulse interval. (D) Mean pulse carrier frequency. (E) Mean root-mean-square (RMS) amplitude.

(F) A composite confocal image of a 28-hr APF pupal ventral nervous system showing *dsx*-expressing neurons (red) labeled with *dsx<sup>Gal4(Δ2)</sup>* (Robinett et al., 2010), and hemilineage 12A neurons (green) of the third subesophageal (S3), and first and second thoracic (T1 and T2) neuromeres labeled with *R24B02.LexA::p65*. All *dsx*-expressing TN1 neurons are among hemilineage 12A neurons in T1 (boxed region, and enlarged in panel below). *dsx<sup>Gal4(Δ2)</sup>*-expressing neurons labeled with an asterisk are part of TN2. Green, GFP; red, dsRed; blue, DNCad. Scale bar represents 100 μm.

(G) The intersection between *R13H01.p65AD::Zp* and *R24B02.Zp::Gdbd* targets neurons of hemilineage 12A in the second (S2) and third (S3) subesophageal, the first (T1) and second (T2) thoracic, and the first (A1) abdominal neuromeres. A composite confocal image is shown of a larval nervous system with GFP labeled in black and DNCad (neuropil) in light gray. Scale bar represents 100 μm.

(H–K) Depletion of *dsx* transcripts in hemilineage 12A (orange) selectively ablates sine song, and causes quantitative defects in pulse song relative to the control (black). (H) The proportion of sine song amount relative to pulse song amount. (I) Mode inter-pulse interval. (J) Mean pulse carrier frequency. (K) Mean RMS amplitude.

(C)–(E) and (I)–(K) show individual points, mean, and SD. Significance was measured using one-way ANOVA with a Tukey-Kramer post hoc test for multiple comparisons. n.s., not significant.

in specific thoracic neurons. *dsx* is expressed in approximately 75 neurons in the male thorax, including two clusters (one on the left side of the nerve cord, one on the right) of approximately 30 interneurons called TN1, which are present in males but not females (Lee et al., 2002; Rideout et al., 2010; Robinett et al., 2010). In both sexes the TN1 neurons are born late during larval development, and subsequently undergo programmed cell death only in females through a *dsx*-dependent mechanism (Rideout et al., 2010; Sanders and Arbeitman, 2008). Most adult neurons in the ventral nervous system are born during larval life from neuronal precursors called neuroblasts (Truman and Bate, 1988). Each neuroblast gives rise to one or two clusters of neurons, called hemilineages (Truman et al., 2004). The location of the TN1 cell bodies and the projection patterns of their neurites are similar to the location and projection patterns of neurons that were previously identified as belonging to the 12A hemilineage in the first thoracic neuromere (Harris et al., 2015). Indeed, a transgenic line, *R24B02-Gal4*, which drives reporter

expression in all immature neurons of hemilineage 12A (Li et al., 2014), drives reporter gene expression in all TN1 neurons, as well as in other neurons of the 12A hemilineage that do not express *dsx* (Figure 1F). *R24B02-Gal4* does not drive reporter gene expression in non-12A hemilineage *dsx*-expressing neurons in the pupal thoracic nervous system, and these other *dsx*-expressing neurons must be derived from other neuronal lineages (Figure 1F).

We sought to test the requirement for (1) the function of *dsx* in hemilineage 12A, and (2) the activity of the TN1 neurons in courtship song. First, we examined the function of *dsx* in hemilineage 12A. If *dsx* function is required specifically in TN1 cells for sine song, then eliminating or reducing the level of *dsx* transcripts in hemilineage 12A (which includes the TN1 cells) should impair sine song. We did not want to test this hypothesis with just the *R24B02-Gal4* line, because this line drives expression in additional neurons outside of the 12A lineage, including other *dsx*-expressing neurons in the brain (not shown). To limit expression

specifically to hemilineage 12A, we exploited the split-Gal4 intersectional approach (Luan et al., 2006; Pfeiffer et al., 2010), which drives expression only in cells at the intersection of two more broadly expressed driver lines. We found that a split-Gal4 intersection between the transgenic lines *R13H01-p65AD::Zp* and *R24B02-Zp::Gdbd* drove reporter expression only in neurons of hemilineage 12A (Figure 1G). We used this split-Gal4 intersection to drive the expression of a validated upstream activating sequence (UAS)-regulated *dsx-ShmiR* (Haley et al., 2008), which depleted *dsx* transcripts in the 12A hemilineage during pupal life. As a control we employed “empty vectors,” in which *R13H01-p65AD::Zp* and *R24B02-Zp::Gdbd* were replaced with identical *p65AD::Zp* and *Zp::Gdbd* transgenic constructs that lacked enhancer fragments. Males with *dsx* downregulated in the 12A hemilineage (*R13H01-p65AD::Zp*  $\cap$  *R24B02-Zp::Gdbd*)>UAS-*dsx-ShmiR*) sang little sine song during courtship, but sang as much pulse song as “empty vector” control flies (Figure 1H). Like *dsx* mutants, males with *dsx* downregulated in the 12A hemilineage (*R13H01-p65AD::Zp*  $\cap$  *R24B02-Zp::Gdbd*)>UAS-*dsx-ShmiR*) sang pulse song with quantitative defects in both the inter-pulse interval and the pulse carrier frequency relative to the control flies (Figures 1I–1K). These results indicate that the 12A hemilineage requires *dsx* function for normal sine and pulse song production. Since the TN1 cells are the only neurons derived from the 12A hemilineage that express *dsx*, these results suggest that some or all TN1 cells require *dsx* function for male flies to produce sine song.

We next asked whether activity of the TN1 neurons is required for courtship song. To test this hypothesis, we targeted just the TN1 neurons using an intersectional strategy based on Flp recombinase (Pfeiffer et al., 2010). We targeted neurons at the intersection of *dsx*-expressing neurons and 12A hemilineage neurons by driving Gal4 in all *dsx*-expressing neurons using *dsx<sup>Gal4(Δ2)</sup>* (Pan et al., 2011; Robinett et al., 2010), and a Flp recombinase in the immature neurons of hemilineage 12A using a *LexA::p65* version of *R13H01*. To visualize the intersected cells, the Flp recombinase excised a transcriptional stop cassette from a UAS-regulated GFP transgene. GFP expression was then driven by the *dsx<sup>Gal4(Δ2)</sup>*. This genetic intersection (*R13H01-LexA::p65*  $\cap$  *dsx<sup>Gal4(Δ2)</sup>*) drove GFP expression in all of the approximately 30 TN1 neurons, with little or no extraneous expression in the brain or ventral nervous system (Figure 2A). The cell bodies of the TN1 neurons are located on the ventral side of the ventral nervous system and project bundled neurites dorsally, where they arborize in the tectulum and wing neuropils to form the “thoracic triangle,” which spans the first and second thoracic neuromeres (Figure 2A).

We used the this intersection (*R13H01-LexA::p65*  $\cap$  *dsx<sup>Gal4(Δ2)</sup>*) to drive the expression of tetanus neurotoxin light chain (*tnt.e*) to suppress the activity of all TN1 neurons (Sweeney et al., 1995; von Philipsborn et al., 2011). As a control, we constructed flies carrying the same genetic intersection driving an inactive form of tetanus neurotoxin (*tnt.QA*). Males expressing the active form of tetanus neurotoxin sang almost no sine song, but sang plentiful pulse song; control flies sang abundant pulse and sine song (Figure 2B). Males with inhibited TN1 neurons produced pulse song with quantitative defects in the inter-pulse interval (Figure 2C), but no defects in the pulse carrier frequency or amplitude (Figures 2D and 2E). We obtained similar results

when we drove a GFP-tagged version of the inwardly rectifying K<sup>+</sup> channel, Kir2.1 (Baines et al., 2001), to inhibit the TN1 neurons (Figures S1A–S1D), instead of the tetanus neurotoxin light chain. These results indicate that TN1 neuronal activity is required for sine song.

A recent study demonstrated that *Drosophila* males modulate their courtship song amplitude according to their distance from a female (Coen et al., 2016). *dsx* mutant males sing pulse song at slightly lower amplitude than wild-type males (Figure 1E). However, depletion of *dsx* transcripts in lineage 12A (Figure 1K) or silencing the TN1 neurons (Figure 2E) in courting males did not appear to affect pulse song amplitude. This suggests that *dsx* regulates pulse song amplitude through cell types other than TN1, potentially including neuronal or somatic cell types.

We next tested whether TN1 activity is sufficient to drive production of sine song by driving neuronal activity specifically in TN1 cells. We expressed the red-shifted channel rhodopsin *csChrimson* (Klapoetke et al., 2014), which depolarizes neurons under red light, in all TN1 neurons. When stimulated with a 15-s bout of red light, these males (*R13H01-LexA::p65*  $\cap$  *dsx<sup>Gal4(Δ2)</sup>*>*csChrimson*) extended and vibrated one wing (Figure S1H) as if they were courting a female, although no female was present. Remarkably, the courtship song induced by red light in these males was composed almost exclusively of sine song (Figures 2F and 2G), with little pulse song (Figures 2H and S1I). The sine song of the TN1-stimulated males was comparable with that of wild-type males (Figure S1J). Taken together, our results demonstrate that *dsx* function is required in the TN1 cluster of neurons for sine song and that activity of the TN1 neurons is both necessary and sufficient for production of sine song.

### TN1 Neurons Are Anatomically Diverse

There are approximately 30 TN1 cells on each side of the ventral nervous system. It is not possible to determine, simply by looking at images of marked TN1 cells, whether all TN1 cells display the same arborization pattern, or whether, in contrast, multiple anatomical types contribute to this cluster of neurons. To differentiate between these alternative hypotheses, we employed a multicolor stochastic labeling technique (Nern et al., 2015) to visualize individual, randomly labeled TN1 neurons. We generated marked cells among the *dsx*-expressing cells and determined that they belonged to the TN1 cluster based on the location of the cell body. Transgenic males were constructed carrying *dsx<sup>Gal4(Δ2)</sup>*, a heat-shock-inducible Flp recombinase, and three separate UAS-regulated transgenes encoding a non-fluorescent GFP protein tagged with either V5, myc, or hemagglutinin (HA) epitopes. Each UAS-regulated transgene contained a transcriptional stop cassette that could be excised by Flp recombinase. A mild heat shock of these flies resulted in stochastic excision of the transcriptional stop cassette from one or more of the three UAS-regulated transgenes. We examined approximately 50 single cell clones and identified five anatomical neuronal subtypes from the TN1 cluster (Figures 3A and 3B). Two TN1 interneuron subtypes, A and B, contribute mainly to the posterior base, which is the dorsal-most region of the thoracic triangle, well within the wing neuropil. Three TN1 interneuron subtypes, C, D, and E, preferentially contribute to the anterior apex of the thoracic triangle. It is possible that the TN1 cluster contains

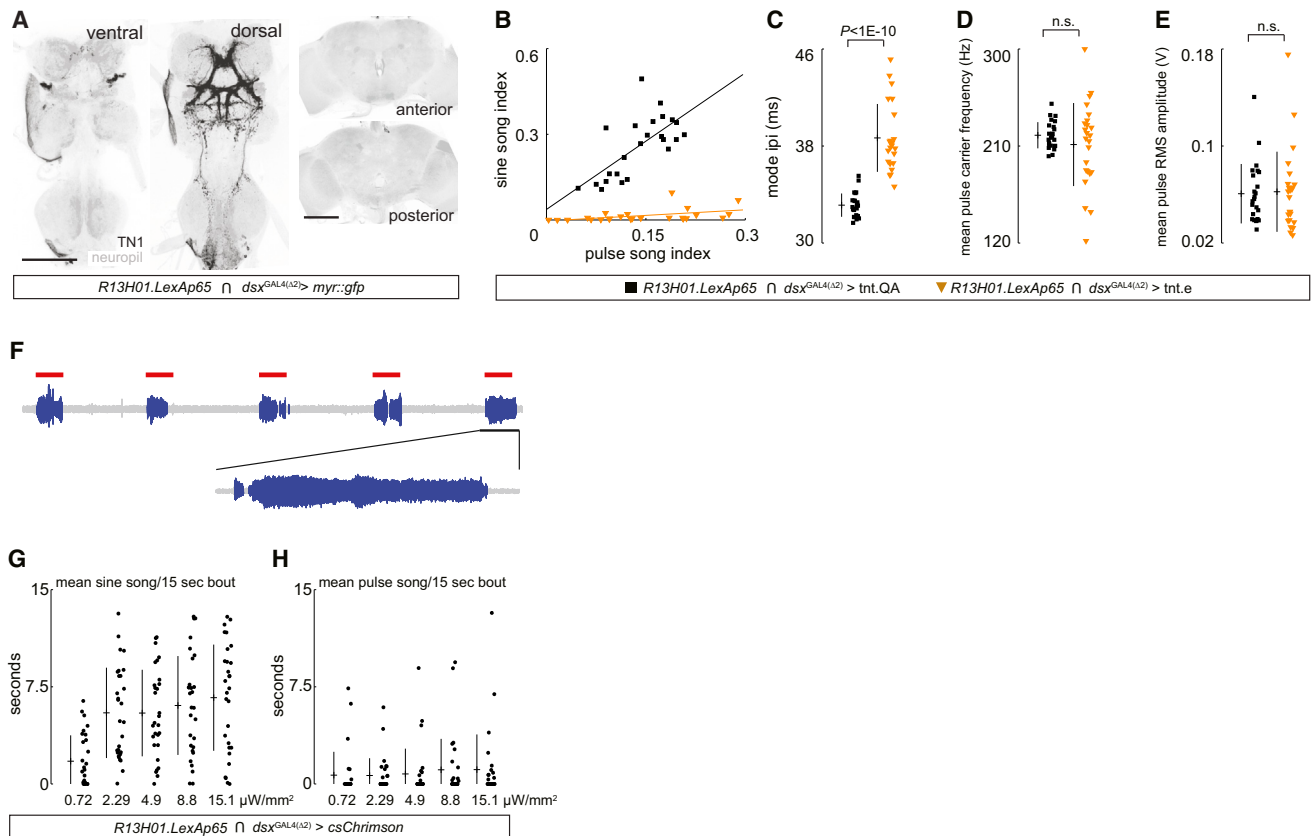


## Figure 2. TN1 Neurons Are Necessary and Sufficient to Induce the Singing of Sine Song

(A) The intersection between  $R13H01.LexA::p65$  and  $dsx^{GAL4(\Delta 2)}$  targets all TN1 neurons in adult males. A composite confocal image is shown with GFP-expressing neurons labeled in black and DNCad (neuropil) in light gray. Scale bar represents 100  $\mu m$ .

(B–E) Courting males with inhibited TN1 neurons using tetanus neurotoxin light chain (orange) are unable to sing sine song, and display quantitative defects in pulse song relative to the control (black). (B) The proportion of sine song amount relative to pulse song amount. (C) Mode inter-pulse interval. (D) Mean pulse carrier frequency. (E) Mean RMS amplitude.

(F–H) *CsChrimson* activation of TN1 neurons preferentially induces the singing of sine song. (F) A clip of courtship song by males expressing *csChrimson* in all TN1 neurons showing five 15-s bouts of red light activation (red bars). Sine song events are labeled in blue, background in gray. (G and H) Amount of sine song (G) or pulse song (H) in seconds per 15-s bout of red light stimulation is shown at noted red light intensities.

(C)–(E), (G), and (H) show individual points, mean, and SD. Significance was measured using one-way ANOVA with a Tukey-Kramer post hoc test for multiple comparisons. n.s., not significant.

additional subtypes that are either rare or simply rarely labeled in this experiment.

### Different TN1 Subtypes Influence Different Aspects of Courtship Song

The anatomical diversity of the TN1 neurons led us to hypothesize that different subtypes contribute to different aspects of courtship song. We therefore searched for and built additional reagents that would allow control of TN1 subtypes; we successfully identified reagents that target two of the five TN1 subtypes. We focus first on subtype TN1A and compare the anatomy and function of the TN1A neurons with the vPR6 thoracic neurons, which were previously reported to influence courtship song (von Philipsborn et al., 2011). Finally, we discuss experiments on TN1C neurons.

We found that the intersection of  $VT017258-Gal4$  (von Philipsborn et al., 2011) with  $dsx^{LexA::p65}$  (Zhou et al., 2015) drove reporter expression in three to six TN1A neurons (Figure S2A).

The intersection between  $VT017258-Gal4$  and  $dsx^{LexA::p65}$  also targeted a *dsx*-expressing interneuron in the second thoracic neuromere called msB (Robinett et al., 2010; Figure S2A), which, unlike the TN1A neurons, is not derived from hemilineage 12A. To target the TN1A neurons specifically and eliminate expression in the msB neurons, we sought to intersect  $VT017258$  and *dsx* with  $R24B02-LexA::p65$ , to restrict expression of the  $VT017258 \cap dsx$  intersection to hemilineage 12A. To accomplish this, we generated a new allele of *dsx* that drives the Gal4 DNA binding domain in the native *dsx* expression pattern. Using CRISPR-Cas9-mediated homology-directed repair (Böttcher et al., 2014; Port et al., 2014), we introduced the Gal4 DNA binding domain fused to a leucine zipper domain ( $Zp::Gdbd$ ) into the *dsx* locus at the start codon within exon 2, creating  $dsx^{Zp::Gdbd}$ . The insertion of this transgene deleted most of *dsx* exon 2, thereby creating a null allele of *dsx* (Figure S2B). To validate the  $dsx^{Zp::Gdbd}$  allele, we intersected  $dsx^{Zp::Gdbd}$  with  $R57C10-p65AD::Zp$ , which targets most or all mature neurons (Jenett

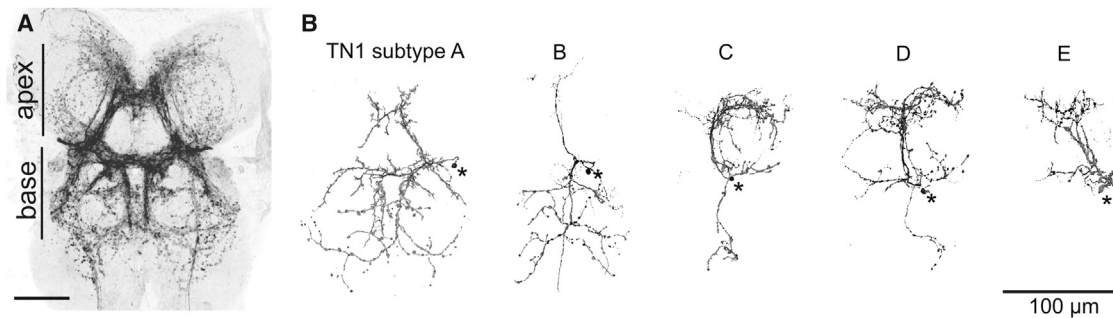


**Figure 3. TN1 Is Composed of Anatomically Diverse Neural Types**

(A) Confocal image showing that the TN1 neurons arborize in the dorsal neuropil to form the “thoracic triangle” spanning the first and second thoracic neuromeres. *R13H01.LexA::p65*  $\cap$  *dsx<sup>Gal4(Δ2)</sup>>myr::gfp* was used to label all 30 TN1 neurons. The anterior apex and posterior base of the triangle are labeled. A composite confocal image is shown with GFP labeled in black and DNCad (neuropil) labeled in light gray. Scale bar represents 100  $\mu$ m.

(B) Single TN1 neurons labeled by the multicolor Flip out technique (Nern et al., 2015) using *dsx<sup>Gal4(Δ2)</sup>* reveals that the TN1 cluster is composed of a variety of anatomical types, five examples of which are shown (TN1 subtypes A–E). The cell body of each neuron is located on the right side of each clone and labeled with an asterisk. Images are reconstructions of single neurons using Amira.

et al., 2012). This intersection recapitulated the expression pattern of *dsx* (Figure S2C), which has been described previously (Rideout et al., 2010; Robinett et al., 2010), including expression in all 30 TN1 neurons, which validates the *dsx<sup>Zp::Gdbd</sup>* allele for our experiments.

Like the *VT017258-Gal4*  $\cap$  *dsx<sup>LexA::p65</sup>* intersection, the intersection between *VT017258-p65AD::Zp* and *dsx<sup>Zp::Gdbd</sup>* drove reporter expression in the TN1A and msB neurons (Figure S2D). As predicted, intersecting *VT017258-p65AD::Zp*  $\cap$  *dsx<sup>Zp::Gdbd</sup>* with the 12A hemilineage driver *R24B02-LexA::p65* drove reporter expression in the TN1A neurons (Figure 4A), but not the msB neurons. It is not clear whether this three-way intersection drives expression in all TN1A cells of the TN1 cluster, but nevertheless it allowed us to test whether TN1A cells contribute to song.

We drove tetanus neurotoxin in the TN1A neurons using (*VT017258-p65AD::Zp*  $\cap$  *dsx<sup>Zp::Gdbd</sup>*)  $\cap$  *R24B02-LexA::p65* and found that courting males sang much less sine song than controls (Figure 4B), but sang normal pulse song (Figures 4C–4E). Neuronal activity of these TN1A neurons is therefore required for normal production of sine song, but not pulse song. However, we cannot rule out the possibility that other TN1A neurons not targeted by this three-way intersection influence pulse song.

We then tested whether activation of TN1A neurons alone is sufficient to drive sine song by driving *csChrimson* with (*VT017258-p65AD::Zp*  $\cap$  *dsx<sup>Zp::Gdbd</sup>*)  $\cap$  *R24B02-LexA::p65* and activating labeled cells with pulses of red light. Whereas activation of the entire TN1 cluster induced sine song, as shown earlier (Figures 2F and 2G), activation of only the TN1A neurons failed to induce much song (Figures S2E–S2G). Therefore, activation of these TN1A cells alone is not sufficient to produce sine song. It is also possible that our intersection does not include all TN1A neurons and that activation of the full complement of TN1A neurons would be, in fact, sufficient to drive sine song. Alternatively, activity of additional TN1 subtypes, either alone or in combination with TN1A, may be required to drive sine song.

The TN1A neurons appear to be anatomically and functionally distinct from the *fru*-expressing vPR6 neurons that were

described previously as contributing to pulse song (von Philipsborn et al., 2011). Intersecting a vPR6 Gal4 line, *VT005534-Gal4* (von Philipsborn et al., 2011), with our hemilineage 12A-expressing line, *R24B02-LexA::p65*, drove reporter expression in the ventral nervous system specifically in the vPR6 neurons, indicating that the vPR6 neurons are derived from hemilineage 12A (Figure S3A). The vPR6 neurons appear similar to TN1A neurons, with arborizations that resemble the posterior base of the thoracic triangle; however, the vPR6 neurons lack arborizations in the anterior apex of the triangle, which TN1A neurons possess (cf. Figures 4A and S3A). Thus, the vPR6 neurons and the TN1A neurons are anatomically distinct hemilineage 12A-derived neurons. We re-examined the role of vPR6 in courtship song using *VT005534-Gal4*  $\cap$  *R24B02-LexA::p65*. Inhibiting vPR6 neurons with tetanus neurotoxin modestly reduced the amount of sine song relative to pulse song (Figure S3B) and significantly increased the pulse carrier frequency relative to the control (Figure S3D). Other song features appeared to be unaffected by inhibition of vPR6 neurons (Figures S3C and S3E). Activating the vPR6 neurons by expressing *csChrimson* in these neurons and exposing flies to pulses of red light induced pulse song (Figures S3F and S3G), consistent with a previous report using thermal activation with *TrpA1* expressed in the vPR6 neurons (von Philipsborn et al., 2011). We observed that activation of vPR6 neurons did not induce sine song (Figure S3H). These data indicate that the vPR6 and TN1A neurons are anatomically and functionally distinct neural classes that primarily influence pulse and sine song, respectively. However, silencing the vPR6 neurons results in a modest reduction in the proportion of sine song (Figure S3B), suggesting that vPR6 neurons also contribute to sine song.

We next studied whether the TN1C neuronal subtype influences song. Zhou et al. (2014) identified a DNA fragment located within the *dsx* locus, *R41A01*, which drives reporter gene expression in a small subset of TN1 neurons and other neurons in the brain. To drive expression in the TN1 neurons specifically, we genetically intersected *R41A01-Gal4* with the hemilineage 12A driver, *R24B02-LexA::p65*. The TN1 neurons targeted in these intersections (Figure 4G) appear to be a single anatomical class that corresponds to TN1C (cf. Figure 3B). Expressing tetanus

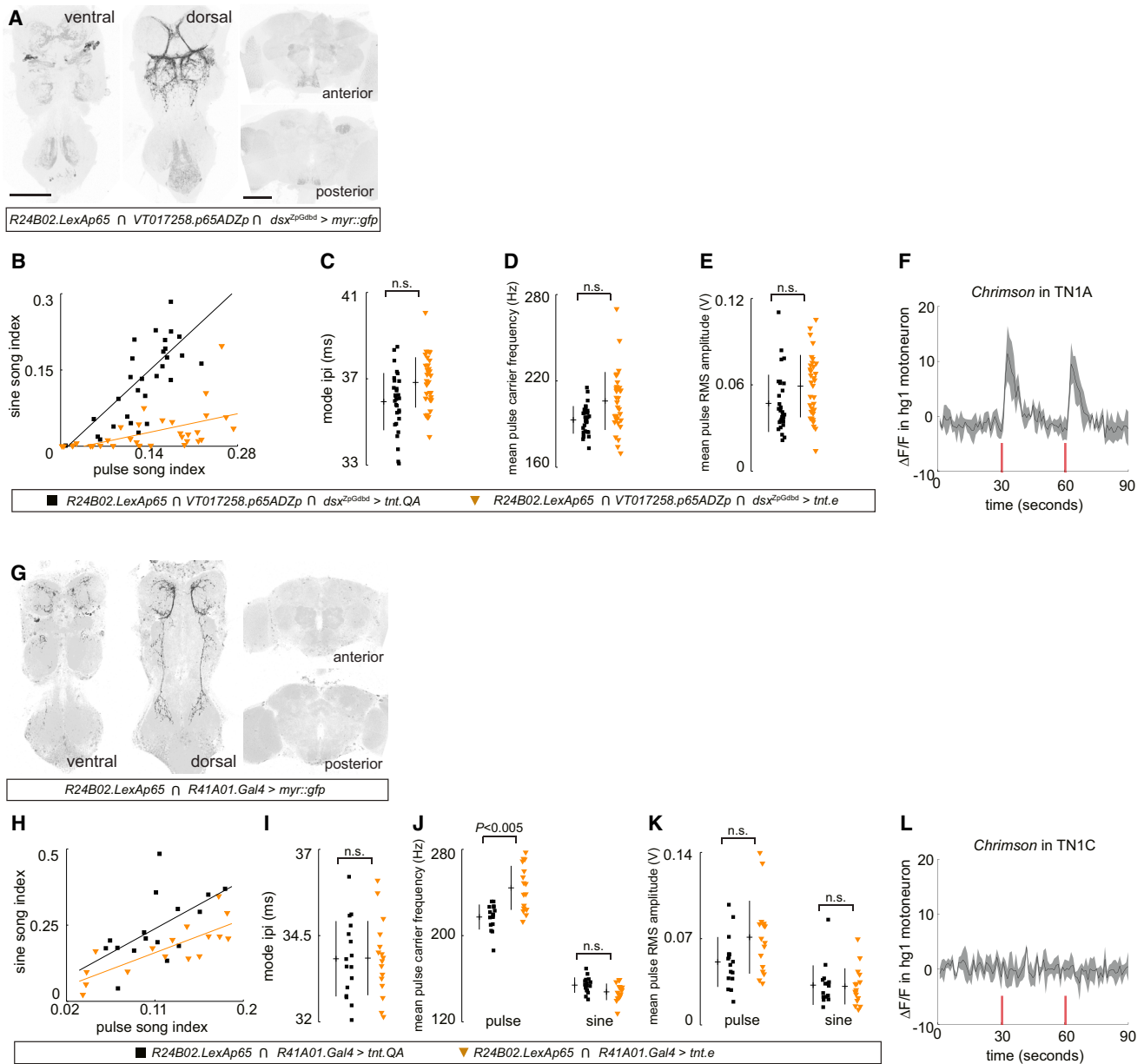


**Figure 4. The Activity of the TN1A Neurons Is Required for the Generation of Sine Song**

(A) A three-way intersection between *R24B02.LexA::p65* and the split-Gal4 intersection between *VT017258.p65AD::Zp* and *dsx<sup>Zp::Gdbd</sup>* targets a subtype of TN1 neurons called TN1A. A composite confocal image is shown with GFP-expressing neurons in black and DNCad (neuropil) in light gray. Scale bar represents 100  $\mu$ m.

(B–E) Courting males with inhibited TN1A neurons using tetanus neurotoxin light chain (orange) sing less sine song relative to the control (black), whereas the pulse song is unaffected. (B) The proportion of sine song amount relative to pulse song amount. (C) Mode inter-pulse interval. (D) Mean pulse carrier frequency. (E) Mean RMS amplitude.

(F) The TN1A neurons and *hg1* motoneuron are functionally coupled. *Chrimson* was expressed in the TN1A neurons using *VT017258.p65AD::Zp*  $\cap$  *dsx<sup>Zp::Gdbd</sup>*, and *GCaMP6s* was expressed in the *hg1* motoneuron using *R52E06.LexA::p65*. Changes in *GCaMP6s* fluorescence intensity in the *hg1* motoneuron was monitored over 90 s. At 30 and 60 s (red bars), a 1-s pulse of red light was directed at the TN1A neurons.

(G) The intersection between *R24B02.LexA::p65* and *R41A01.Gal4* targets a subtype of TN1 neurons that correspond to TN1C. A composite confocal image is shown with GFP-expressing neurons in black and DNCad (neuropil) in light gray. Scale bar represents 100  $\mu$ m.

(H–K) Courting males with inhibited TN1C neurons (orange) display a variety of song defects relative to the control (black). (H) The proportion of sine song amount relative to pulse song amount. (I) Mode inter-pulse interval. (J) Mean pulse carrier frequency. (K) Mean RMS amplitude.

(L) TN1C neurons and the *hg1* motoneuron are not functionally linked. The same experimental protocol was used as the one described in (F), except *R41A01.LexA::p65* was used to express *Chrimson* in the TN1C neurons.

(C)–(E) and (I)–(K) show individual points, mean, and SD. In (F) and (L),  $n = 8$  sides. Mean  $\Delta F/F$  and SD is plotted. Significance was measured using one-way ANOVA with a Tukey-Kramer post hoc test for multiple comparisons. n.s., not significant.

neurotoxin in the TN1C neurons resulted in a slight reduction in the amount of sine song relative to pulse song (Figure 4H) and an increase in the pulse carrier frequency (Figure 4J). These effects are similar to those observed by inhibiting the vPR6 neurons (Figures 4H–4K) and suggest that the TN1C and vPR6 neurons may contribute to the same neural circuit. Considering all of these results together, we conclude that at least some anatomically distinct TN1 subtypes influence different aspects of courtship song.

### The TN1A Neurons Are Functionally Linked to the *hg1* Motoneuron

We sought to determine whether the TN1A neurons are functionally connected to other neurons required for sine song. We found previously that the motoneuron that innervates the sexually dimorphic wing muscle, *hg1*, is required for the generation of sine song but not pulse song (Shirangi et al., 2013). Given that the TN1A neurons and the *hg1* motoneuron both contribute to the generation of sine song, we hypothesized that the two neuronal types are functionally linked. To test this, we expressed *csChrimson* in the TN1A neurons using *VT017258-p65AD::Zp*  $\cap$  *dsx<sup>Zp::Gdbd</sup>*, and a fluorescent calcium sensor, *GCaMP6s* (Chen et al., 2013), in the *hg1* motoneuron using *R52E06-LexA::p65*. As a control, we expressed *csChrimson* in the TN1C neurons, driven by *R41A01-Gal4*. Using explanted ventral nervous systems, we activated the TN1A or TN1C neurons specifically by using a digital micromirror device to shine red light focused on the respective neurons for 1 s at 30 and 60 s during a 90-s trial. We measured calcium transients in the *hg1* motoneuron as changes in *GCaMP6s* fluorescence. The *hg1* motoneuron displayed a strong increase in *GCaMP6s* fluorescence immediately after activation of TN1A neurons, indicating that TN1A neurons and the *hg1* motoneuron are functionally coupled (Figure 4F). In contrast, activation of the TN1C neurons did not increase *GCaMP6s* fluorescence in the *hg1* motoneuron (Figure 4L). Therefore, the TN1A neurons, but not the TN1C neurons, are functionally connected to the *hg1* motoneuron, consistent with the fact that both the TN1A neurons and the *hg1* motoneuron are required for sine song.

### Doublesex Regulates the Functional Link between the TN1A Neurons and *hg1* Motoneuron

The experiments described above demonstrated that the TN1A neurons (which express *dsx*) are functionally coupled to the *hg1* motoneuron (which does not express *dsx*) (Shirangi et al., 2013), and that both neurons are required for sine song. Given that *dsx* mutant males are unable to sing sine song (Vilella and Hall, 1996), we hypothesized that *dsx* may regulate the functional linkage between TN1A neurons and the *hg1* motoneuron. We therefore tested whether the connectivity between the TN1A neurons and the *hg1* motoneuron is altered in the absence of *dsx* function. As before, we used *VT017258-p65AD::Zp*  $\cap$  *dsx<sup>Zp::Gdbd</sup>* to express *csChrimson* in the TN1A neurons and *R52E06-LexA::p65* to express *GCaMP6s* in the *hg1* motoneuron. Now, however, we tested the functional connectivity between these neurons in a *dsx* null background and when *dsx* transcripts were knocked down specifically in the TN1A neurons.

We first tested whether *dsx* is required for specification and survival of TN1A neurons. We found that *dsx* null males produce

the same number of TN1A neurons, marked with the genetic intersection *VT017258-p65AD::Zp*  $\cap$  *dsx<sup>Zp::Gdbd</sup>*, as control males that were heterozygous for a *dsx* null allele (Figures 5J and 5K). Therefore, *dsx* is not required for specification or survival of TN1A neurons.

We then tested the functional connectivity between TN1A neurons and the *hg1* motoneuron in the absence of *dsx* expression. We found that activation of the TN1A neurons in the control *dsx* heterozygote males resulted in rapid and strong increases in *GCaMP6s* fluorescence in the *hg1* motoneuron (Figure 5A). In contrast, in *dsx* null males, we found that stimulation of TN1A neurons resulted in only a minor increase in *GCaMP6s* fluorescence in the *hg1* motoneuron (Figure 5B). These results indicate that *dsx* is required for the strong functional connection between TN1A neurons and the *hg1* motoneuron.

To determine whether this connectivity requires *dsx* function specifically in the TN1A neurons, we repeated the experiment, but used *VT017258-p65AD::Zp*  $\cap$  *dsx<sup>Zp::Gdbd</sup>* to express the *dsx-ShmiR* to deplete *dsx* transcripts more specifically in the TN1A neurons. After activation of TN1A neurons, control flies, which did not contain the *dsx-ShmiR*, produced strong *GCaMP6s* fluorescence in the *hg1* motoneuron (Figure 5C), but flies with *dsx* depleted in the TN1A neurons produced no detectable increase in *GCaMP6s* fluorescence in the *hg1* motoneuron (Figure 5D). These data suggest that *dsx* acts in the TN1A neurons to regulate their functional connections with the *hg1* motoneuron. The loss of the functional connection between TN1A neurons and the *hg1* motoneuron in *dsx* mutants likely explains why *dsx* mutant males are unable to sing sine song.

### Doublesex Is Not Required during Adulthood for the Generation of Sine Song

*dsx* could regulate the functional connection between the TN1A neurons and the *hg1* motoneuron by influencing the morphological development of the TN1A neurons during pupal life, or by influencing the physiology of the TN1A neurons during adulthood, or both. To distinguish between these possibilities, we tested whether *dsx* is required for sine song after adult flies eclose from the puparium. We conditionally depleted *dsx* transcripts in adult males using a tubulin promoter to drive temperature-sensitive Gal80 (*TubP-Gal80<sup>TS</sup>*) (McGuire et al., 2003) with *dsx<sup>Gal4(Δ2)</sup>-UAS-dsx-ShmiR*. At the permissive temperature (18°C), Gal80<sup>TS</sup> represses Gal4 activation of gene expression. At the restrictive temperature (29°C), Gal80<sup>TS</sup> is inactivated and allows Gal4 to activate gene expression. As a control, we used the empty *attP2* landing site in place of the *UAS-dsx-ShmiR* transgene. Flies were placed at the permissive temperature (18°C) to repress the expression of *dsx-ShmiR* throughout embryonic, larval, and pupal development. After eclosion, males were shifted to the restrictive temperature (29°C), at which they were maintained for 8 days, resulting in the expression of *dsx-ShmiR* and depletion of *dsx* transcripts. To confirm that we successfully depleted *dsx* transcripts during adulthood, we immunostained ventral nervous systems from *TubP-Gal80<sup>TS/+</sup>;dsx<sup>Gal4(Δ2)</sup>/UAS-dsx-ShmiR*, *attP2* and control *TubP-Gal80<sup>TS/+</sup>;dsx<sup>Gal4(Δ2)</sup>/attP2* male flies with an anti-DSX antibody (Mellert et al., 2012). Dsx protein expression was undetectable in any *dsx*-expressing neurons, including TN1, in *TubP-Gal80<sup>TS/+</sup>;dsx<sup>Gal4(Δ2)</sup>/UAS-dsx-ShmiR*, *attP2* ventral nervous

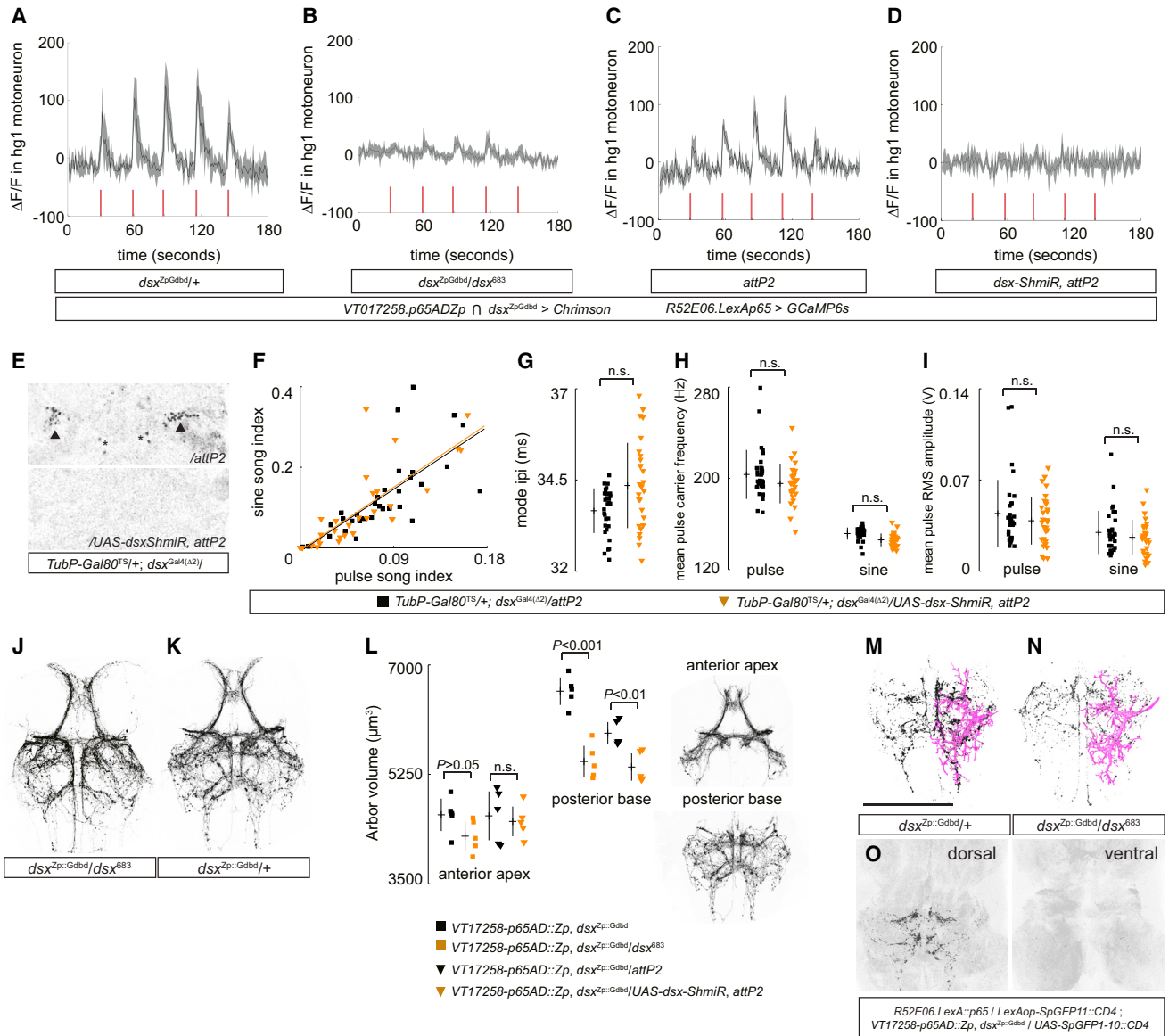


**Figure 5. *dsx* Regulates the Link between the TN1A Neurons and *hg1* Motoneuron**

(A–D) The functional link between the TN1A neurons and *hg1* motoneuron is strongly attenuated in *dsx* mutant males and in males expressing *dsx-ShmiR* in the TN1A neurons. Changes in *GCaMP6s* fluorescence intensity in the *hg1* motoneuron is shown over the course of 180 s in (A) *dsx* heterozygote control, (B) *dsx* null, (C) *attP2* control, and (D) *UAS-dsx-ShmiR, attP2* males whose TN1A neurons were *Chrimson* activated with 1-s stimulations of red light at 0.12, 0.24, 0.48, 1.2, and 0.12 mW/mm<sup>2</sup> intensities at approximately 30, 60, 90, 120, and 150 s, respectively. (A and B) n = 4 sides each. (C and D) n = 7 sides each. A t test was used to compare the mean  $\Delta F/F$  of the experimental males (B and D) with the mean  $\Delta F/F$  of their respective controls (A and C) during the first 5 s following each pulse of red light. For each period, p < 0.03.

(E–I) *dsx* expression is not required during adulthood for sine song production. *TubP-Gal80<sup>TS/+</sup>; dsx<sup>Gal4(Δ2)/attP2</sup>* males (control) and *TubP-Gal80<sup>TS/+</sup>; dsx<sup>Gal4(Δ2)/UAS-dsx-ShmiR, attP2</sup>* males were all raised throughout development at the permissive temperature, 18°C. At eclosion, males were transferred to the restrictive temperature, 29°C, and aged for 8–10 days to allow for the depletion of *dsx* transcripts during adulthood by expression of *dsx-ShmiR*. (E) Expression of male-specific *Dsx* protein is observed in the TN1 neurons of *attP2* (control), but not that of *UAS-dsx-ShmiR, attP2* males. (F–I) Courtship song of *TubP-Gal80<sup>TS/+</sup>; dsx<sup>Gal4(Δ2)/UAS-dsx-ShmiR, attP2</sup>* males (orange) is largely unaffected relative to that of *TubP-Gal80<sup>TS/+</sup>; dsx<sup>Gal4(Δ2)/attP2</sup>* males (black). (F) The proportion of sine song amount relative to pulse song amount. (G) Mode inter-pulse interval. (H) Mean pulse carrier frequency. (I) Mean RMS amplitude.

(J and K) The number and gross anatomy of the TN1A neurons is unaffected in *dsx* mutant males. The intersection between *R24B02.LexA::p65* and the split-Gal4 intersection, *VT017258.p65AD::Zp dsx<sup>Zp::Gdbd</sup>*, was used to visualize the TN1A neurons in *dsx* heterozygote control (K) and *dsx* null (J) males. *dsx* heterozygote control (K) males have 11.8 ± 1.1 cells (n = 6), and *dsx* null (J) males have 12.1 ± 0.75 cells (n = 6).

(L) The arbor volume of the TN1A neurons' posterior base is significantly reduced in *dsx* mutant and *dsx-ShmiR*-expressing males (orange) relative to controls (black), whereas the arbor volume of the anterior apex is largely unaffected.

(legend continued on next page)

systems, but we detected Dsx protein expression in control *TubP-Gal80<sup>TS/+</sup>;dsx<sup>Gal4(Δ2)/attP2</sup>* ventral nervous systems (Figure 5E). Nevertheless, the absence of *dsx* expression in TN1 and other *dsx*-expressing neurons during adulthood did not substantially alter either the quantity or quality of sine and pulse song (Figure 5F), with the exception of the inter-pulse interval, which displayed a modest increase in mean and variance relative to the control (Figures 5G–5I). These results suggest that *dsx* is required prior to eclosion for the generation of sine song. Since *dsx* is first expressed in hemilineage 12A during pupal development (Sanders and Arbeitman, 2008), *dsx* probably influences TN1A neuronal development and connectivity to the *hg1* motoneuron during pupal development.

### Doublesex Regulates the Density of the TN1A Neurons' Arbors that Likely Interact with the Dendrites of the *hg1* Motoneuron

The experiments described above indicate that the linkage between the TN1A neurons and the *hg1* motoneuron requires *dsx* function. This connection is most likely established during pupal development, when the TN1A neurons terminally differentiate. We therefore hypothesized that *dsx* regulates the anatomical development of the TN1A neurons to allow functional coupling with the *hg1* motoneuron.

To test this hypothesis, we examined the arborization pattern of the TN1A neurons in the presence and absence of *dsx* activity. We visualized the TN1A neurons using *VT017258-p65AD::Zp*  $\cap$  *dsx<sup>Zp::Gdbd</sup>* in *dsx* null and *dsx* heterozygote (control) males, and found that the gross morphology of the TN1A neurons was similar in *dsx* mutant (Figure 5J) and control (Figure 5K) males. However, relative to control males, *dsx* mutant males displayed a substantial reduction in the volume of the dorsal-most arbors of the TN1A neurons that contribute to the posterior base of the thoracic triangle (Figure 5L). The volume of the TN1A neurons' arbors that supply the anterior apex of the triangle, however, was similar in *dsx* null and *dsx* heterozygote males (Figure 5L). We observed a similar reduction in arbor density when *dsx* transcripts were depleted more specifically in the TN1A neurons by using *VT017258-p65AD::Zp*  $\cap$  *dsx<sup>Zp::Gdbd</sup>* to drive *dsx-ShmiR* (Figure 5L), suggesting that these phenotypes are caused by a cell-autonomous requirement for *dsx* in the TN1A neurons. These results demonstrate that *dsx* is required for normal growth and development of the TN1A arbors that supply the posterior base of the thoracic triangle.

The posterior base of the TN1A neurons is positioned within the wing neuropil, where wing motoneurons extend dendrites. Thus, the posterior base of TN1A neurons may make synaptic contacts with the dendrites of the *hg1* motoneuron in this region. To test this, we labeled the TN1A neurons and the *hg1* motoneuron with different markers in individual males using *VT017258-p65AD::Zp*  $\cap$  *dsx<sup>Zp::Gdbd</sup>* and *R52E06-LexA::p65*, respectively. We found that the arbors of the posterior base of

the TN1A neurons are intertwined closely and extensively with a subset of the *hg1* motoneuron's dendritic arbors (Figure 5M and Movie S1). The arbors of the posterior base that are reduced in *dsx* mutants include those that are intertwined with the dendrites of the *hg1* motoneuron (Figure 5N). To determine whether the overlap in arbors between TN1A neurons and the *hg1* motoneuron are potentially synaptic, we utilized GRASP (GFP Reconstitution Across Synaptic Partners) (Feinberg et al., 2008; Gordon and Scott, 2009), in which two halves of GFP were separately expressed in either TN1A neurons or the *hg1* motoneuron using *VT017258-p65AD::Zp*  $\cap$  *dsx<sup>Zp::Gdbd</sup>* and *R52E06-LexA::p65*, respectively. If the arbors of TN1A neurons and the *hg1* motoneuron are close enough for synaptic contact, then GFP fluorescence should be reconstituted. Indeed, we found reconstitution of GFP specifically in the posterior base of the TN1A neurons, where the arbors of TN1A neurons and the *hg1* motoneuron are predicted to interact based on co-labeling data (Figure 5O). These data suggest that TN1A neurons and the *hg1* motoneuron are synaptic partners, in addition to being functionally connected; however, electron microscopy is required to confirm physical synapses between TN1A neurons and the *hg1* motoneuron.

## DISCUSSION

We have discovered that the *dsx* gene establishes a functional connection between a class of male-specific interneurons—the TN1A neurons—and a sex-non-specific wing motoneuron, *hg1*. The TN1A neurons and the *hg1* motoneuron contribute specifically to sine song. During pupal development, the TN1A neurons begin to express *dsx* (Sanders and Arbeitman, 2008), which promotes an increase in the density of the dorsal-most arbors of the TN1A neurons. These arbors appear to contact and make synaptic connections with dendrites of the *hg1* motoneuron. The functional and anatomical connection between the TN1A and *hg1* neurons most likely facilitates the generation of sine song during male courtship. Our results illustrate how a sexual differentiation regulatory gene can build a circuit element for a sex-specific motor behavior using sex-specific (TN1A) and sex-non-specific (*hg1*) neurons.

While the TN1 neurons are necessary and sufficient for the singing of sine song, other sine song circuit elements in the thoracic nervous system probably exist. For instance, artificial activation of *fru*-P1-expressing neurons in females, which lack TN1, induced singing of both pulse and sine song (Clyne and Miesenböck, 2008). This suggests that the female nervous system contains neurons whose artificial activation is capable of inducing sine song even in the absence of TN1 neurons. The identity of these neurons is currently unknown.

Our findings also demonstrate that a variety of circuit motifs can arise from a single neuronal lineage in the ventral nervous system. Most neurons in the adult fly ventral nervous system

(M and N) The TN1A neurons' posterior base (black) are intertwined extensively with the dendrites of the *hg1* motoneuron (magenta) in *dsx* heterozygote control (M) and *dsx* mutant (N) males, but the arbor density of the TN1A neurons is reduced in *dsx* mutants relative to the control. *VT017258.p65AD::Zp*  $\cap$  *dsx<sup>Zp::Gdbd</sup>* was used to label the TN1A neurons, and the *hg1* motoneuron was stochastically labeled with *R52E06.LexA::p65*. The TN1A neurons' posterior base and the *hg1* motoneuron were segmented and reconstructed in Amira. Scale bar in (M) represents 100  $\mu$ m.

(O) A GRASP signal (black) is detected where the TN1A neurons and *hg1* motoneuron is predicted to interact based on co-labeling data (M).

Significance in (A)–(D), (F)–(I), and (L) was measured using one-way ANOVA with a Tukey-Kramer post hoc test for multiple comparisons. n.s., not significant.

are born during larval life from neuronal precursors called neuroblasts (Truman and Bate, 1988). Each neuroblast gives rise to one or two clusters of neurons, called hemilineages (Truman et al., 2004). The neurons within each hemilineage tend to develop similar arborization patterns (Truman et al., 2004) and contribute to specific, different subsets of adult fly behaviors (Harris et al., 2015; Truman et al., 2004). For example, neurons of hemilineage 12A innervate the dorsal neuropil of the ventral nervous system, including the tectulum and the wing neuropil, and thus arborize in appropriate locations to regulate wing movements (Shepherd et al., 2016). Many hemilineage 12A neurons develop in similar ways in males and females and contribute to various wing movements (Harris et al., 2015), whereas others, such as the TN1 neurons, are present in males but not females and contribute specifically to male courtship song. Thus, the 12A hemilineage contains neurons with different functions. Some neurons contribute to neural circuits in both sexes while others influence sex-specific wing behaviors such as song. Previous studies have shown that the adult ventral nervous system is “modular” and that neurons in different hemilineages have different adult functions (Harris et al., 2015). Our results reveal that this modularity extends even deeper: individual hemilineages contain neurons that pattern distinct, yet related behaviors.

The modular organization of the 12A hemilineage extends even to different male-specific neurons that influence distinct features of courtship song. For example, whereas the TN1A subclass of 12A neurons contributes to sine song but not pulse song, the vPR6 and TN1C subclasses preferentially influence pulse song. Our previous study on the neuromuscular control of courtship song revealed that the wing musculature is also functionally modular: different wing muscles influence different features of song (Shirangi et al., 2013). Thus, the neuronal circuits that drive pulse and sine song appear to be non-overlapping, at least from thoracic circuits to the wing musculature. It is possible that there are also distinct pulse and sine pathways descending from the brain that drive the pulse and sine circuits in the ventral nervous system. Flies normally sing sine and pulse song in non-overlapping patterns, and it will be interesting to identify the circuits that allow switching between pulse and sine song.

Courtship songs are exceedingly diverse among species of the genus *Drosophila* and many species do not sing sine song (D.L.S. and T.R.S., unpublished data). In at least some species, such as those closely related to *D. melanogaster*, sine song was probably secondarily lost during evolution. Ancestral species may not have sung sine song. The neural circuit controlling sine song may have evolved between these species to generate divergent songs. Here we have described at least some of the circuitry that drives sine song. Are the TN1A neurons present in species that do not sing sine song, and if so, how do their anatomy and function differ? This question can be addressed by developing neurogenetic tools in divergent drosophilids to allow anatomical and functional studies of neural circuits in other *Drosophila* species.

## EXPERIMENTAL PROCEDURES

### Fly Stocks

Flies were reared on standard cornmeal and molasses food at 25°C. The stocks used in this paper include the following: Canton S, *dsx*<sup>Gal4(Δ2)</sup>

(Pan et al., 2011); *dsx*<sup>LexA::p65</sup> (Zhou et al., 2015), *UAS-FRT>STOP>FRT-tnt.QA* and *UAS-FRT>STOP>FRT-tnt.e* (von Philipsborn et al., 2011); *pBPhsFlp2::PEST* (attP3) and *pJFRC201-10XUAS-FRT>STOP>FRT-myr::smGFP-HA* (VK0005); *pJFRC240-10XUAS-FRT>STOP>FRT-myr::smGFP-V5-THS-10XUAS-FRT>STOP>FRT-myr::smGFP-FLAG* (su(Hw)attP1) (Nern et al., 2015); *R41A01.Gal4* (attP2) (Zhou et al., 2014); *VT005534.Gal4*, *VT017258.Gal4* (attP2) (von Philipsborn et al., 2011); *TubP-Gal80<sup>TS</sup>* (McGuire et al., 2003); *LexAop-SpGFP11::CD4/CyO*; and *UAS-SpGFP1-10::CD4/TM6B* (Gordon and Scott, 2009). *dsx*<sup>1</sup> was kindly provided by B. Baker (Janelia). *dsx*<sup>683</sup> (i.e., *Df(3R)00683-d07058*; Chatterjee et al., 2011) was a gift from C. Robinett (Janelia). *R13H01.p65AD::Zp* (attP40), *R24B02.Zp::Gdbd* (attP2), *pBP.p65AD::Zp* (attP40), *pBP.Zp::Gdbd* (attP2), *R13H01.LexA::p65* (attP40), *R24B02.LexA::p65* (attP40), *R24B02.Gal4* (attP2), *pJFRC79-8XLexAop2-FlpL* (attP40), *20XUAS-FRT>STOP>FRT-CsChrimson-mVenus* (attP2), *pJFRC56-10XUAS-FRT>STOP>kir2.1::gfp* (attP2), *pJFRC41-10XUAS-FRT>STOP>FRT-myr::gfp* (su(Hw)attP1), *pJFRC21-10XUAS-IVS-mCD8::RFP* (su(Hw)attP8), *pJFRC15-13XLexAop2-mCD8::gfp* (attP18), *R57C10.p65AD::Zp* (attP40), *R52E06.LexA::p65* (attP40), *pJFRC220-13XLexAop2-KDRT>STOP>KDRT-myr::smGFP-FLAG* (su(Hw)attP5), and *pJFRC12-10XUAS-IVS-myr::gfp* (attP2) were gifts from G. Rubin (Janelia). *VT017258.p65AD::Zp* (attP2) was kindly provided by B. Dickson (Janelia). *HS-KD1* (attP18) was kindly provided by T. Lee (Janelia). *13XLexAop2-IVS-Syn21-OpGCaMP6s-p10* (su(Hw)attP8) (Chen et al., 2013) and *10XUAS-IVS-Syn21-Chrimson::ttd-3.1* (attP18) were generated by B. Pfeiffer and described in Hooper et al. (2015). *P[y[+7.7]=CaryP]attP2* and *P[y[+7.7]v[+1.8]=TRiP.GLV21010]attP2* (i.e., *UAS-dsx-ShmiR*) were obtained from the *Drosophila* Transgenic RNAi Project at Harvard Medical School.

### Immunohistochemistry

Nervous systems were dissected in PBS and fixed in 4% paraformaldehyde (buffered in PBS) for 35 min at room temperature. Fixed tissues were washed in PBT (PBS with 1% Triton X-100), blocked in PBT-NGS (PBT with 3% normal goat serum) for 1 hr, and incubated with primary antibodies diluted in PBT-NGS overnight at 4°C. Tissues were washed in PBT at room temperature for several hours, and incubated overnight at 4°C with secondary antibodies in PBT-NGS. Tissues were washed all day in PBT, placed onto polylysine-coated coverslips, dehydrated through an ethanol series, cleared in xylenes, and mounted in DPX (Sigma-Aldrich). Most tissues were imaged on a Zeiss LSM 510 confocal microscope at 40x with optical sections usually at 0.4-μm intervals. The following primary antibodies were used: mouse anti-DSX (1:200) (Mellert et al., 2012), rabbit anti-GFP (Life Technologies #A11122; 1:1,000), rat anti-FLAG (Novus Biologicals #NBP1-06712; 1:200), rabbit anti-HA (Cell Signaling Technologies #3724S; 1:300), DyLight549-conjugated mouse anti-V5 (AbD Serotec #MCA1360D549; 1:300), mouse anti-GFP (Sigma #G6539; 1:100), rat anti-DN-cadherin (DN-Ex #8, Developmental Studies Hybridoma Bank; 1:50), and rabbit anti-DsRed (Clontech #632496; 1:500). The MultiColor FlpOut experiments (Nern et al., 2015) were performed by crossing males from a stock carrying *dsx*<sup>Gal4(Δ2)</sup> to virgin females carrying *pBPhsFlp2::PEST* (attP3), *pJFRC201-10XUAS-FRT>STOP>FRT-myr::smGFP-HA* (VK0005), and *pJFRC240-10XUAS-FRT>STOP>FRT-myr::smGFP-V5-THS-10XUAS-FRT>STOP>FRT-myr::smGFP-FLAG* (su(Hw)attP1). Males of the appropriate genotype were collected soon after eclosion, heat-shocked at 37°C for 5 min, and subsequently aged for 5–7 days at 25°C before being taken for dissection and staining with antibodies against FLAG, V5, and MYC epitopes. To co-label the TN1A neurons and a single *hg1* motoneuron in individual males (as shown in Figures 5M and 5N), we crossed males carrying *R52E06.LexA::p65*, *pJFRC220-13XLexAop2-KDRT>STOP>KDRT-myr::smGFP-FLAG*, *VT017258.p65AD::Zp* and *dsx*<sup>Zp::Gdbd</sup> to virgin females carrying *HS-KD1* and *pJFRC12-10XUAS-IVS-myr::gfp*. Males of the appropriate genotype were collected at eclosion, heat-shocked at 37°C for 5 min, and subsequently aged for 5–7 days before being taken for dissection and staining. Reconstructions (shown in Figures 3B, 5M, and 5N) were done using Amira (Visualization Sciences Group). Confocal stacks were imported into Amira, neurons of interest were segmented and reconstructed by selecting and assigning pixels through the confocal series to labels of their respective neuron. Amira was also used to measure neuronal arbor volume (as shown in Figure 5L) using the appropriate voxel dimensions (in μm).

### Construction of *dsx<sup>Zp::Gal4</sup>*

CRISPR-Cas9 homology-directed repair (HDR) was used to insert the Gal4 DNA binding domain (DBD) into the ATG of the first coding exon of *dsx*. An HDR plasmid was constructed using Gibson assembly (Gibson et al., 2009) of the following PCR fragments: the origin of replication and ampicillin resistance gene from pBR322, the Gal4DBD from pBPZpGal4DBDUw, and a 1,796-bp left-hand homology arm and a 1,913-bp right-hand homology arm from the *dsx* locus. This plasmid was co-injected with in vitro transcribed mRNA of a codon-optimized Cas9 gene and a Dicer-substrate small interfering RNA targeting the *lig4* gene (sequence 1: rUrCrCrUrGrCrArGrCrUrGrArUrGrCrUrUrGr rCrUrG rUrGrU rCrGrU; sequence 2: rGrArC rArCrA rGrCrA rArGrC rArUrC rArGrC rUrGrC rArGG A, synthesized by IDT), to suppress non-homologous end-joining following DNA breakage (Böttcher et al., 2014). Guide RNAs (gRNAs) internally flanking the homology arms were cloned into pCFD4 (Port et al., 2014). Embryos of *w<sup>1118</sup>* flies were injected by Rainbow Transgenic Flies using the following concentrations: 0.5 μg/μl gRNA plasmid, 0.5 μg/μl donor DNA, 0.1 μg/μl Cas9 mRNA, and 0.1 μg/μl *lig4* small interfering RNA.

### Functional Imaging

We collected flies of the stated genotype and dissected the ventral nerve cord (VNC) in *Drosophila* adult saline containing 103 mM NaCl, 3 mM KCl, 5 mM TES (2-[tris(hydroxymethyl)-methylamino]-ethanesulfonic acid), 8 mM trehalose dihydrate, 10 mM glucose, 26 mM NaHCO<sub>3</sub>, 1 mM NaH<sub>2</sub>PO<sub>4</sub>, 2 mM CaCl<sub>2</sub>, and 4 mM MgCl<sub>2</sub>, and bubbled with carbogen. After dissection, the VNC was gently adhered to a polylysine-coated coverslip and placed underneath the imaging objective. We perfused the sample with saline at 21°C. Volume imaging was performed on a resonant scanning, piezo 2-photon microscope at 235 × 235 × 84 μm (at 0.92 Hz). We imaged at 920 nm to avoid activating *Chrimson* with the imaging wavelength. *Chrimson* was activated with a 660-nm LED (M660L3 Thorlabs) coupled to a digital micromirror device (Texas Instruments DLPC300 Light Crafter) to deliver light to specific cells. Fluorescence signal was measured at the cell body of the *hg1* motoneuron and quantified.

### Recording and Analysis of Courtship Song

Newly eclosed males were collected under CO<sub>2</sub> and individually housed for 4–7 days (unless otherwise noted) at 25°C and 30%–50% humidity with a 12-hr light/dark cycle. Virgin *Canton S* females were group-housed and aged under similar conditions. Courtship song was recorded as described by Shirangi et al. (2013) for 10–15 min at 25°C within 2 hr after the start of the subjective day using individual pairs of males and decapitated females. In experiments using *TubP-Gal80<sup>TS</sup>*, progeny from a cross between males carrying *P[y[+7.7]=CaryP]attP2* (control) or *P[y[+7.7] v[+1.8]=TRiP.GLV21010] attP2* (*UAS-dsx-ShmiR*) and virgin females carrying *TubP-Gal80<sup>TS</sup>* and *dsx<sup>Gal4(Δ2)</sup>* were reared at 18°C throughout development until eclosion. Males of the appropriate genotype were collected, housed individually, and aged for 8–10 days at 29°C. Courtship song was subsequently recorded at 25°C. All courtship song recordings were analyzed using MATLAB R2013 as described previously (Shirangi et al., 2013). Only gaps shorter than 100 ms were analyzed to measure the inter-pulse interval. *Chrimson* experiments were performed in the dark. Males were recorded without the presence of a female. Red light was delivered using a NIDAQ board. Males were stimulated four times with 15 s of continuous red light at each intensity for four times. Each stimulation was followed by 45 s of no light.

### SUPPLEMENTAL INFORMATION

Supplemental Information includes three figures and one movie and can be found with this article online at <http://dx.doi.org/10.1016/j.devcel.2016.05.012>.

### AUTHOR CONTRIBUTIONS

T.S., A.W., J.T., and D.S. performed experiments and wrote the paper.

### ACKNOWLEDGMENTS

We thank J. Cande, J. Crocker, Y. Ding, A. Korgaonkar, J. Lillis, J. Mast, E. Preger-Ben Noon, and R. Sen for helpful discussions; B. Baker, J. Cande,

and two reviewers for comments on the manuscript; B. Pfeiffer, G. Rubin, and D. Anderson for the design, construction, and gift of the *csChrimson* and *OpGCAMP6s* stocks; S.S. Kim for the software to control the digital micromirror device; C. Morkunas and M. Radcliff for administrative assistance; and the TRiP at Harvard Medical School (NIH/NIGMS R01-GM084947) for providing transgenic RNAi fly stocks. This work was supported by the Howard Hughes Medical Institute.

Received: March 7, 2016

Revised: May 6, 2016

Accepted: May 18, 2016

Published: June 20, 2016

### REFERENCES

- Baines, R.A., Uhler, J.P., Thompson, A., Sweeney, S.T., and Bate, M. (2001). Altered electrical properties in *Drosophila* neurons developing without synaptic transmission. *J. Neurosci.* 21, 1523–1531.
- Baker, B.S., Taylor, B.J., and Hall, J.C. (2001). Are complex behaviors specified by dedicated regulatory genes? Reasoning from *Drosophila*. *Cell* 105, 13–24.
- Billeter, J.-C., Rideout, E.J., Dorman, A.J., and Goodwin, S.F. (2006). Control of male sexual behavior in *Drosophila* by the sex determination pathway. *Curr. Biol.* 16, R766–R776.
- Böttcher, R., Hollmann, M., Merk, K., Nitschko, V., Obermaier, C., Philippou-Massier, J., Wieland, I., Gaul, U., and Förstemann, K. (2014). Efficient chromosomal gene modification with CRISPR/cas9 and PCR-based homologous recombination donors in cultured *Drosophila* cells. *Nucleic Acids Res.* 42, e89.
- Cachero, S., Ostrovsky, A.D., Yu, J.Y., Dickson, B.J., and Jefferis, G.S.X.E. (2010). Sexual dimorphism in the fly brain. *Curr. Biol.* 20, 1589–1601.
- Chatterjee, S.S., Uppendahl, L.D., Chowdhury, M.A., Ip, P.-L., and Siegal, M.L. (2011). The female-specific doublesex isoform regulates pleiotropic transcription factors to pattern genital development in *Drosophila*. *Development* 138, 1099–1109.
- Chen, T.-W., Wardill, T.J., Sun, Y., Pulver, S.R., Renninger, S.L., Baohan, A., Schreiter, E.R., Kerr, R.A., Orger, M.B., Jayaraman, V., et al. (2013). Ultrasensitive fluorescent proteins for imaging neuronal activity. *Nature* 499, 295–300.
- Clyne, J.D., and Miesenböck, G. (2008). Sex-specific control and tuning of the pattern generator for courtship song in *Drosophila*. *Cell* 133, 354–363.
- Coen, P., Xie, M., Clemens, J., and Murthy, M. (2016). Sensorimotor transformations underlying variability in song intensity during *Drosophila* courtship. *Neuron* 89, 629–644.
- Feinberg, E.H., VanHoven, M.K., Bendesky, A., Wang, G., Fetter, R.D., Shen, K., and Bargmann, C.I. (2008). GFP Reconstitution across Synaptic Partners (GRASP) defines cell contacts and synapses in living nervous systems. *Neuron* 57, 353–363.
- Gibson, D.G., Young, L., Chuang, R.-Y., Venter, J.C., Hutchison, C.A., and Smith, H.O. (2009). Enzymatic assembly of DNA molecules up to several hundred kilobases. *Nat. Methods* 6, 343–345.
- Gordon, M.D., and Scott, K. (2009). Motor control in a *Drosophila* taste circuit. *Neuron* 61, 373–384.
- Haley, B., Hendrix, D., Trang, V., and Levine, M. (2008). A simplified miRNA-based gene silencing method for *Drosophila melanogaster*. *Dev. Biol.* 321, 482–490.
- Harris, R.M., Pfeiffer, B.D., Rubin, G.M., and Truman, J.W. (2015). Neuron hemilineages provide the functional ground plan for the *Drosophila* ventral nervous system. *Elife* 4, <http://dx.doi.org/10.7554/eLife.04493>.
- Hoopfer, E.D., Jung, Y., Inagaki, H.K., Rubin, G.M., and Anderson, D.J. (2015). P1 interneurons promote a persistent internal state that enhances inter-male aggression in *Drosophila*. *Elife* 4, <http://dx.doi.org/10.7554/eLife.11346>.
- Jenett, A., Rubin, G.M., Ngo, T.T.B., Shepherd, D., Murphy, C., Dionne, H., Pfeiffer, B.D., Cavallo, A., Hall, D., Jeter, J., et al. (2012). A GAL4-driver line resource for *Drosophila* neurobiology. *Cell Rep.* 2, 991–1001.

- Klapoetke, N.C., Murata, Y., Kim, S.S., Pulver, S.R., Birdsey-Benson, A., Cho, Y.K., Morimoto, T.K., Chuong, A.S., Carpenter, E.J., Tian, Z., et al. (2014). Independent optical excitation of distinct neural populations. *Nat. Methods* **11**, 338–346.
- Kohl, J., Ostrovsky, A.D., Frechter, S., and Jefferis, G.S.X.E. (2013). A bidirectional circuit switch reroutes pheromone signals in male and female brains. *Cell* **155**, 1610–1623.
- Lee, G., Foss, M., Goodwin, S.F., Carlo, T., Taylor, B.J., and Hall, J.C. (2000). Spatial, temporal, and sexually dimorphic expression patterns of the fruitless gene in the *Drosophila* central nervous system. *J. Neurobiol.* **43**, 404–426.
- Lee, G., Hall, J.C., and Park, J.H. (2002). Doublesex gene expression in the central nervous system of *Drosophila melanogaster*. *J. Neurogenet.* **16**, 229–248.
- Li, H.H., Kroll, J.R., Lennox, S.M., Ogundeyi, O., Jeter, J., Depasquale, G., and Truman, J.W. (2014). A GAL4 driver resource for developmental and behavioral studies on the larval CNS of *Drosophila*. *Cell Rep.* **8**, 897–908.
- Luan, H., Peabody, N.C., Vinson, C., and White, B.H. (2006). Refined spatial manipulation of neuronal function by combinatorial restriction of transgene expression. *Neuron* **52**, 425–436.
- Manoli, D.S., Foss, M., Villella, A., Taylor, B.J., Hall, J.C., and Baker, B.S. (2005). Male-specific fruitless specifies the neural substrates of *Drosophila* courtship behaviour. *Nature* **436**, 395–400.
- Manoli, D.S., Meissner, G.W., and Baker, B.S. (2006). Blueprints for behavior: genetic specification of neural circuitry for innate behaviors. *Trends Neurosci.* **29**, 444–451.
- Manoli, D.S., Fan, P., Fraser, E.J., and Shah, N.M. (2013). Neural control of sexually dimorphic behaviors. *Curr. Opin. Neurobiol.* **23**, 330–338.
- McGuire, S.E., Le, P.T., Osborn, A.J., Matsumoto, K., and Davis, R.L. (2003). Spatiotemporal rescue of memory dysfunction in *Drosophila*. *Science* **302**, 1765–1768.
- Mellert, D.J., Robinett, C.C., and Baker, B.S. (2012). Doublesex functions early and late in gustatory sense organ development. *PLoS One* **7**, e51489.
- Nern, A., Pfeiffer, B.D., and Rubin, G.M. (2015). Optimized tools for multicolor stochastic labeling reveal diverse stereotyped cell arrangements in the fly visual system. *Proc. Natl. Acad. Sci. USA* **112**, E2967–E2976.
- Pan, Y., Robinett, C.C., and Baker, B.S. (2011). Turning males on: activation of male courtship behavior in *Drosophila melanogaster*. *PLoS One* **6**, e21144.
- Pfeiffer, B.D., Ngo, T.-T.B., Hibbard, K.L., Murphy, C., Jenett, A., Truman, J.W., and Rubin, G.M. (2010). Refinement of tools for targeted gene expression in *Drosophila*. *Genetics* **186**, 735–755.
- Port, F., Chen, H., Lee, T., and Bullock, S.L. (2014). Optimized CRISPR/Cas tools for efficient germline and somatic genome engineering in *Drosophila*. *Proc. Natl. Acad. Sci. USA* **111**, E2967–E2976.
- Portman, D.S. (2007). Genetic control of sex differences in *C. elegans* neurobiology and behavior. *Adv. Genet.* **59**, 1–37.
- Rideout, E.J., Billeter, J.-C., and Goodwin, S.F. (2007). The sex-determination genes fruitless and doublesex specify a neural substrate required for courtship song. *Curr. Biol.* **17**, 1473–1478.
- Rideout, E.J., Dornan, A.J., Neville, M.C., Eadie, S., and Goodwin, S.F. (2010). Control of sexual differentiation and behavior by the doublesex gene in *Drosophila melanogaster*. *Nat. Neurosci.* **13**, 458–466.
- Robinett, C.C., Vaughan, A.G., Knapp, J.M., and Baker, B.S. (2010). Sex and the single cell. II. there is a time and place for sex. *PLoS Biol.* **8**, e1000365.
- Sanders, L.E., and Arbeitman, M.N. (2008). Doublesex establishes sexual dimorphism in the *Drosophila* central nervous system in an isoform-dependent manner by directing cell number. *Dev. Biol.* **320**, 378–390.
- Shepherd, D., Harris, R., Williams, D., and Truman, J.W. (2016). Postembryonic lineages of the *Drosophila* ventral nervous system: neuroglial expression reveals the adult hemilineage associated fiber tracts in the adult thoracic neuromeres. *J. Comp. Neurol.* <http://dx.doi.org/10.1002/cne.23988>.
- Shirangi, T.R., Stern, D.L., and Truman, J.W. (2013). Motor control of *Drosophila* courtship song. *Cell Rep.* **5**, 678–686.
- Stockinger, P., Kvitsiani, D., Rotkopf, S., Tirián, L., and Dickson, B.J. (2005). Neural circuitry that governs *Drosophila* male courtship behavior. *Cell* **121**, 795–807.
- Sweeney, S.T., Brodie, K., Keane, J., Niemann, H., and O’Kane, C.J. (1995). Targeted expression of tetanus toxin light chain in *Drosophila* specifically eliminates synaptic transmission and causes behavioral defects. *Neuron* **14**, 341–351.
- Truman, J.W., and Bate, M. (1988). Spatial and temporal patterns of neurogenesis in the central nervous system of *Drosophila melanogaster*. *Dev. Biol.* **125**, 145–157.
- Truman, J.W., Schuppe, H., Shepherd, D., and Williams, D.W. (2004). Developmental architecture of adult-specific lineages in the ventral CNS of *Drosophila*. *Development* **131**, 5167–5184.
- Villella, A., and Hall, J.C. (1996). Courtship anomalies caused by doublesex mutations in *Drosophila melanogaster*. *Genetics* **143**, 331–344.
- von Philipsborn, A.C., Liu, T., Yu, J.Y., Masser, C., Bidaye, S.S., and Dickson, B.J. (2011). Neuronal control of *Drosophila* courtship song. *Neuron* **69**, 509–522.
- Yu, J.Y., Kanai, M.I., Demir, E., Jefferis, G.S.X.E., and Dickson, B.J. (2010). Cellular organization of the neural circuit that drives *Drosophila* courtship behavior. *Curr. Biol.* **20**, 1602–1614.
- Zhou, C., Pan, Y., Robinett, C.C., Meissner, G.W., and Baker, B.S. (2014). Central brain neurons expressing doublesex regulate female receptivity in *Drosophila*. *Neuron* **83**, 149–163.
- Zhou, C., Franconville, R., Vaughan, A.G., Robinett, C.C., Jayaraman, V., and Baker, B.S. (2015). Central neural circuitry mediating courtship song perception in male *Drosophila*. *Elife* **4**, <http://dx.doi.org/10.7554/eLife.08477>.

Developmental Cell, Volume 37

**Supplemental Information**

***Doublesex* Regulates the Connectivity of a Neural  
Circuit Controlling *Drosophila* Male Courtship Song**

**Troy R. Shirangi, Allan M. Wong, James W. Truman, and David L. Stern**

## Supplemental Figures and legends

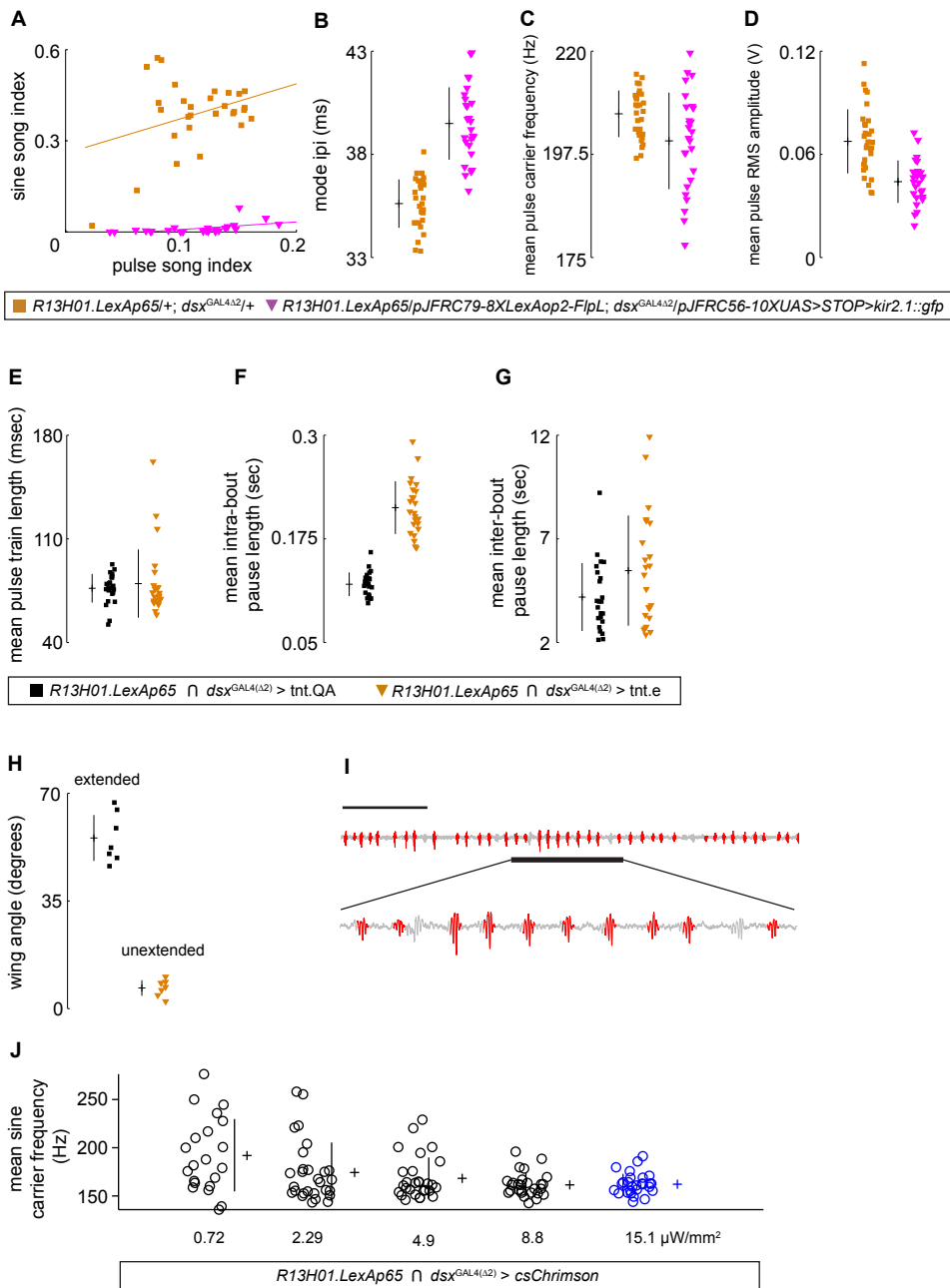


**Figure S1. Related to Figure 2.** The intersection between *R13H01.LexA::p65* and *dsx<sup>Gal4(Δ2)</sup>* was used to express *kir2.1::gfp* in all TN1 neurons in courting males. **(A)** The proportion of sine song amount relative to pulse song amount. **(B)** Mode inter-pulse interval. **(C)** Mean pulse carrier frequency. **(D)** Mean rms amplitude. **(E)** Mean pulse train length of males with inhibited TN1 neurons (orange) is statistically equivalent relative to the control (black). **(F)** Mean intra-bout pause length is greater in males with inhibited TN1 neurons (orange) relative to the control (black) due to the selective loss of sine song. **(G)** Mean inter-pause length of males with inhibited TN1 neurons (orange) is statistically equivalent relative to the control (black). **(H)** *csChrimson* activation of TN1 neurons induces a single wing extension. The angle of both wings was measured in a single video frame within the first three bouts of red light stimulation. Every male examined ( $n=7$ ) extended one wing for the duration of the stimulus at an average of 55.4 degrees, whereas the other wing remained relatively unextended at an average of 6.7 degrees. **(I)** An example of pulse song generated by a *csChrimson*-TN1-activated male. Pulses are in red. **(J)** *csChrimson* activation of the TN1 neurons produces a sine song with a carrier frequency comparable to wild-type *D. melanogaster* males (i.e., 160 Hz).

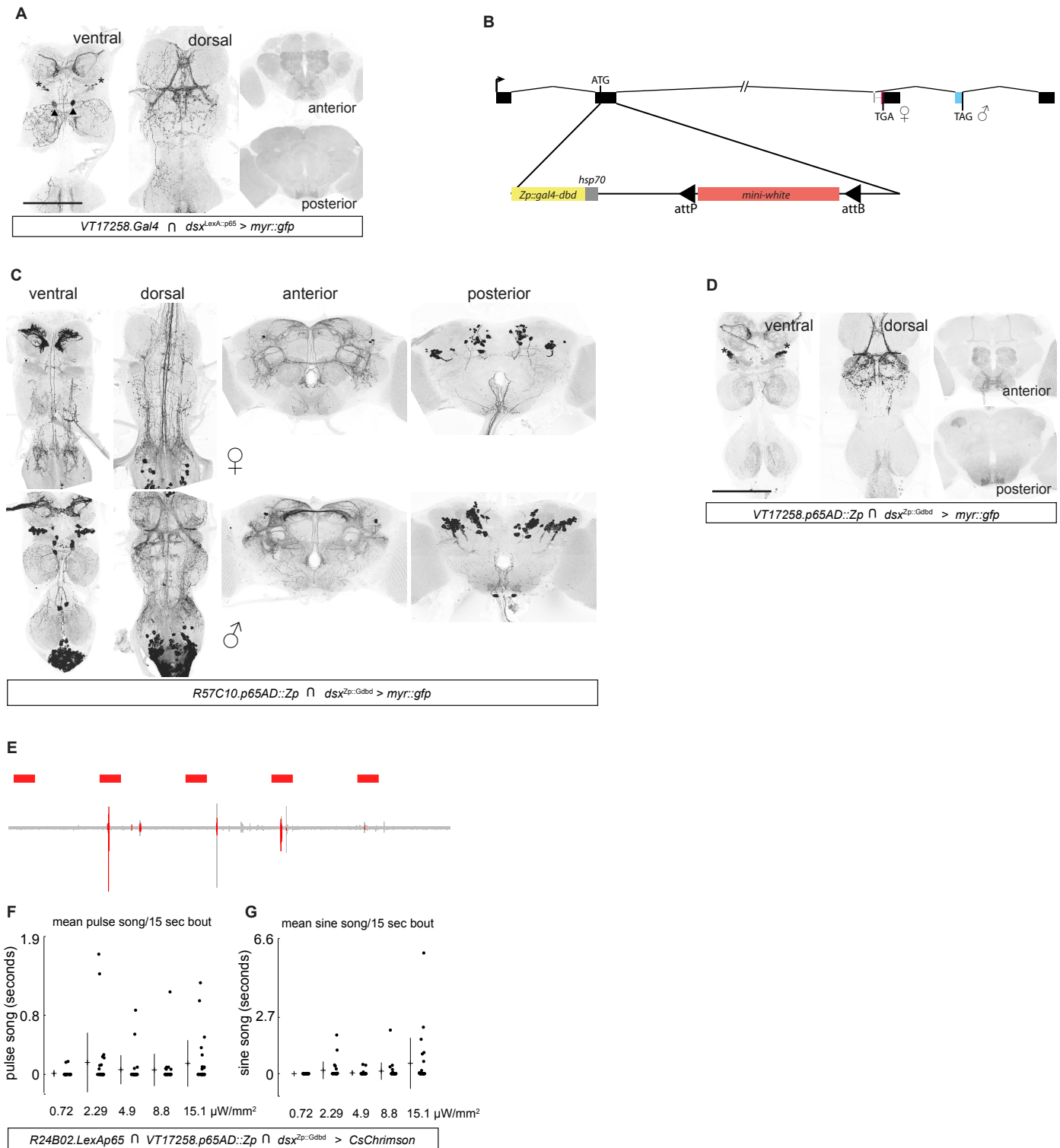


**Figure S2. Related to Figure 4.** (A) Intersection between *VT017258.Gal4* and *dsx<sup>LexA:p65</sup>* targets the TN1A subtype of TN1 neurons (asterisk) and the *dsx*-expressing msB neuron (arrowheads). (B) Design of *dsx<sup>Zp-Gdbd</sup>*. (C) Intersection of *R57C10.p65AD::Zp* and *dsx<sup>Zp-Gdbd</sup>* faithfully recapitulates *dsx* expression in the CNS as reported elsewhere (Robinett et al., 2011; Rideout et al., 2011). (D) The intersection between *VT017258.p65AD::Zp* and *dsx<sup>Zp-Gdbd</sup>* targets the TN1A neurons (asterisk) and the msB neurons (weakly targeted in this intersection). (E-G) *csChrimson* activation of the TN1A neurons in males does not induce a significant amount of pulse or sine song. Audio recordings of males expressing *csChrimson* in TN1A neurons showing five 15-second bouts of red light activation (red bars). Pulse song events are labeled in red, sine song in blue, background in gray. Amount of pulse (F) song or sine (G) song in seconds per 15-second bout of red light stimulation is shown at 0.72, 2.29, 4.9, 8.8 and 15.1  $\mu\text{W}/\text{mm}^2$  red light intensities. Panels A, C and D are composite confocal images of adult nervous systems with GFP-expressing neurons labeled in black and DNCad (neuropil) labeled in light gray.

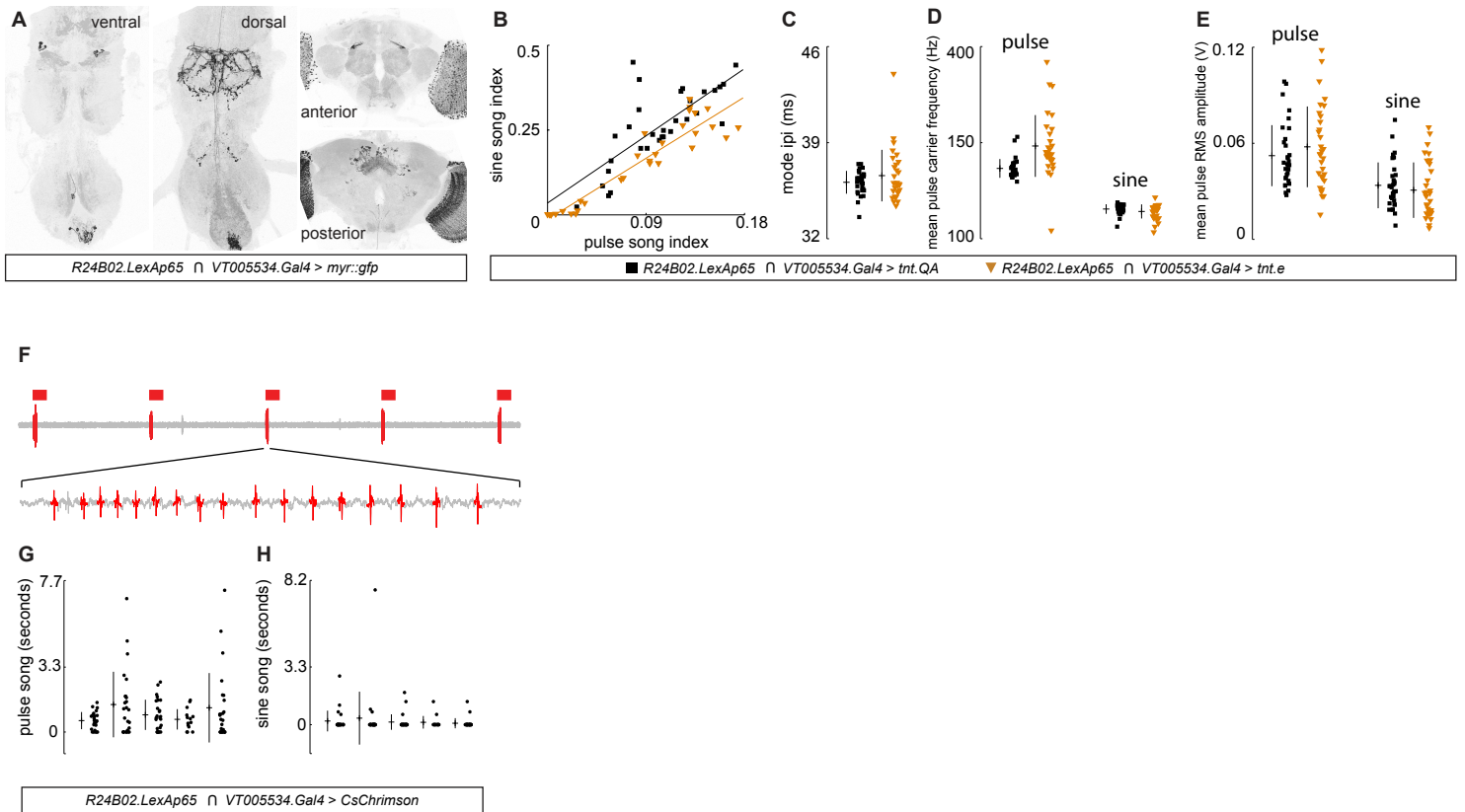


**Figure S3. Related to Figure 4.** (A) Intersection between *R24B02.LexA::p65* and *VT005534.Gal4* targets the vPR6 neurons. Composite confocal image of an adult nervous system is shown with GFP-expressing neurons labeled in black and DNCad (neuopil) labeled in light gray. (B-E) Inhibition of vPR6 neurons in courting males. (B) The proportion of sine song amount relative to pulse song amount. (C) Mode inter-pulse interval. (D) Mean pulse carrier frequency. (E) Mean rms amplitude. (F-H) *csChrimson* activation of vPR6 neurons in courting males preferentially induces pulse song. (F) Song produced by males expressing *csChrimson* in vPR6 neurons and exposed to five 15-second bouts of red light (red bars). Pulse song events are labeled in red, background in gray. Amount of pulse (G) or sine (H) song in seconds per 15-second bout of red light stimulation is shown at 0.72, 2.29, 4.9, 8.8 and 15.1  $\mu\text{W}/\text{mm}^2$  red light intensities. (C-E) and (G, H) show individual points, the mean and SD.

**Movie S1. Related to Figure 5.** Reconstruction of the TN1A neurons (posterior base only; white) and the hg1 motoneuron (magenta).